Supporting Information

The Role of Solvent-Molecule Hydrogen Bonding in Polyphenylfluorene-Carbazole Systems: Tuning Molecular Packing Patterns, Crystal Morphologies, and Solid-State Luminescence Efficiency

Yi Tan[a], Yan Li[a], Haoran Li[a], Shuting Xie[a], Yang Li[a], Cheng Yang[a], Jingyao Ma[a], Jingrui Zhang[a], Zheng Zhang[a], Lingzhi Jin[a], Yugang Chen[a], Kuande Wang[a], Zhihao Xue[a], Yihao Mu[a], Jiangtian Tan[*,a], Shasha Wang[*,a], and Linghai Xie[*,a]

[a] Centre for Molecular Systems and Organic Devices (CMSOD), State Key Laboratory of Flexible Electronics (LoFE) & Institute of Advanced Materials (IAM), Nanjing University of Posts & Telecommunications, 9 Wenyuan Road, Nanjing 210023, China.

[b] School of Electronics Information Engineering & School of Integrated Circuits, Nanjing University of Industry Technology, Nanjing 210023, China

[*] Joint corresponding authors.

E-mail addresses: 403747@njupt.edu.cn (J. Tan), iamsswang@njupt.edu.cn (S. Wang), iamlhxie@njupt.edu.cn (L. Xie).

Content:

This PDF file includes:

Figure S1-S16.

Table S1-S5.

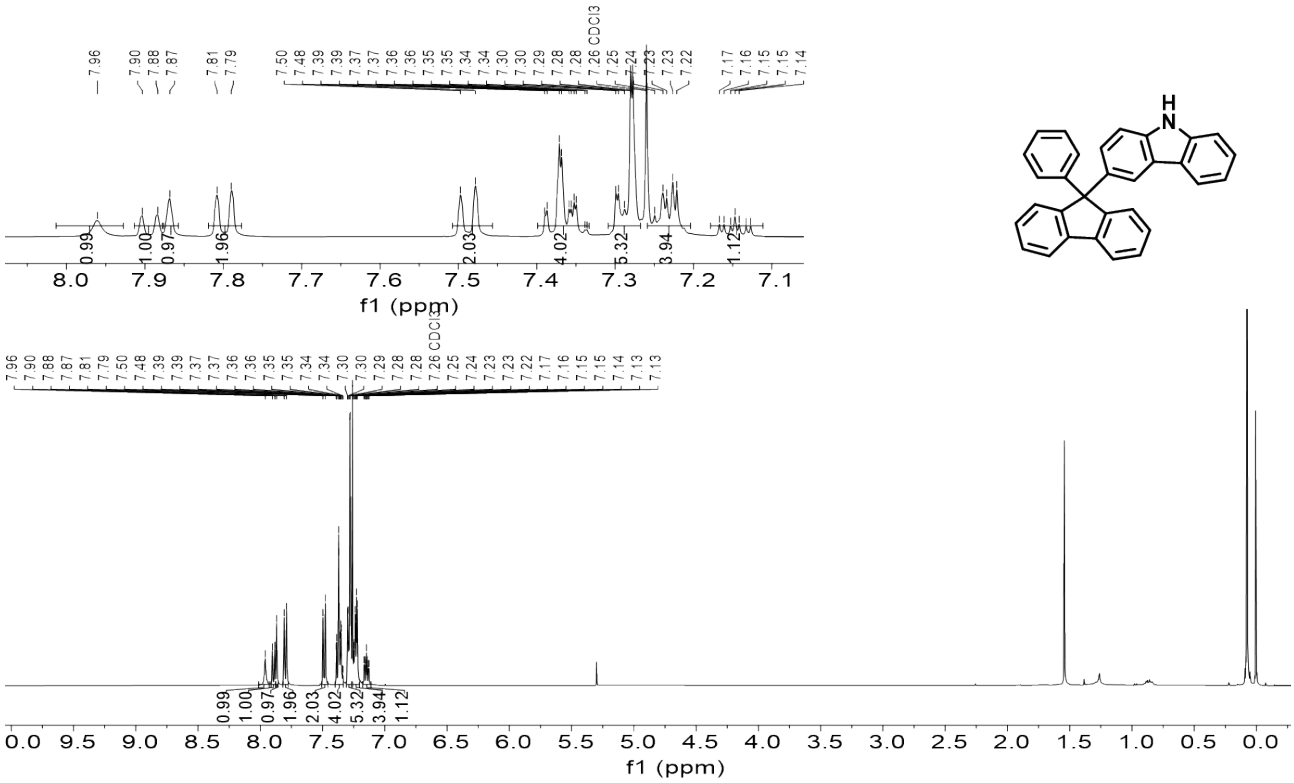

Figure S1. ^{1}H NMR spectrum of PFCz recorded in $CDCl_3$.

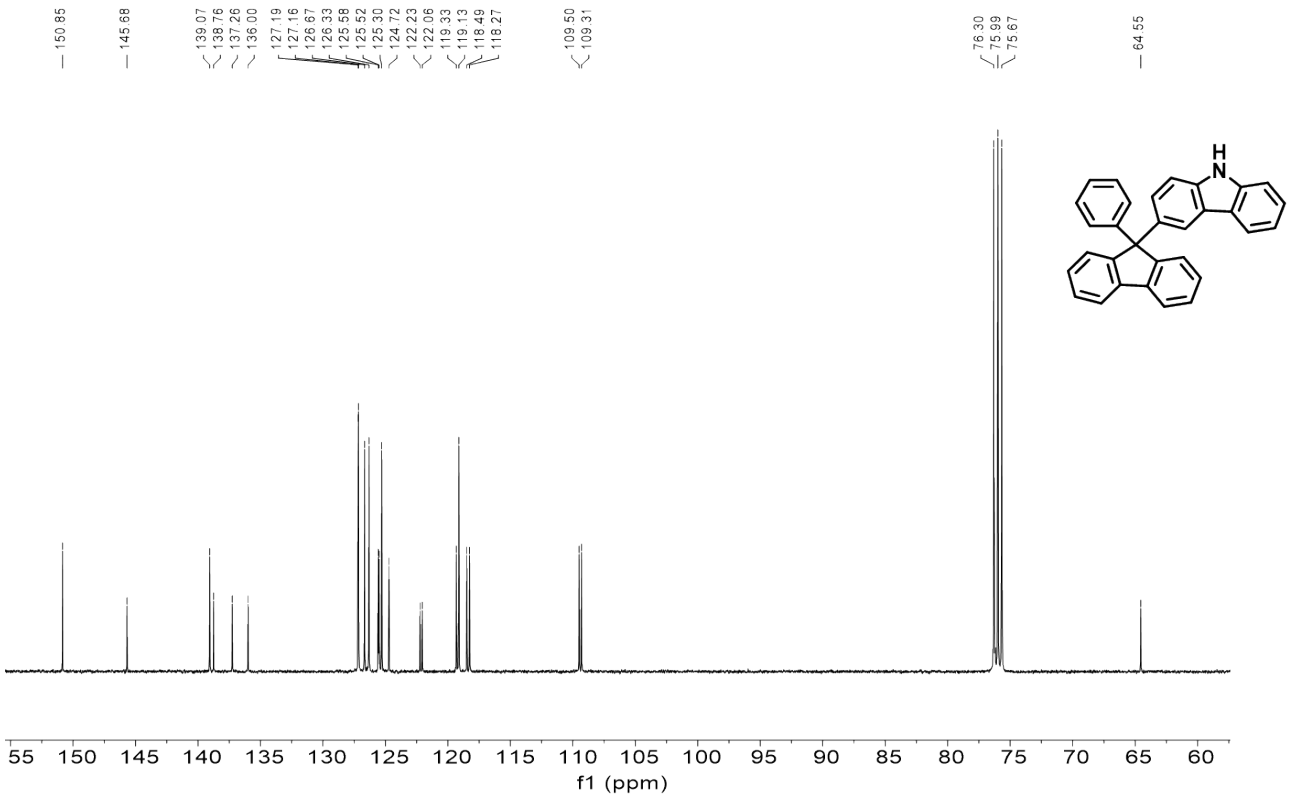

Figure S2. ^{13}C NMR spectrum of PFCz recorded in $CDCl_3$.

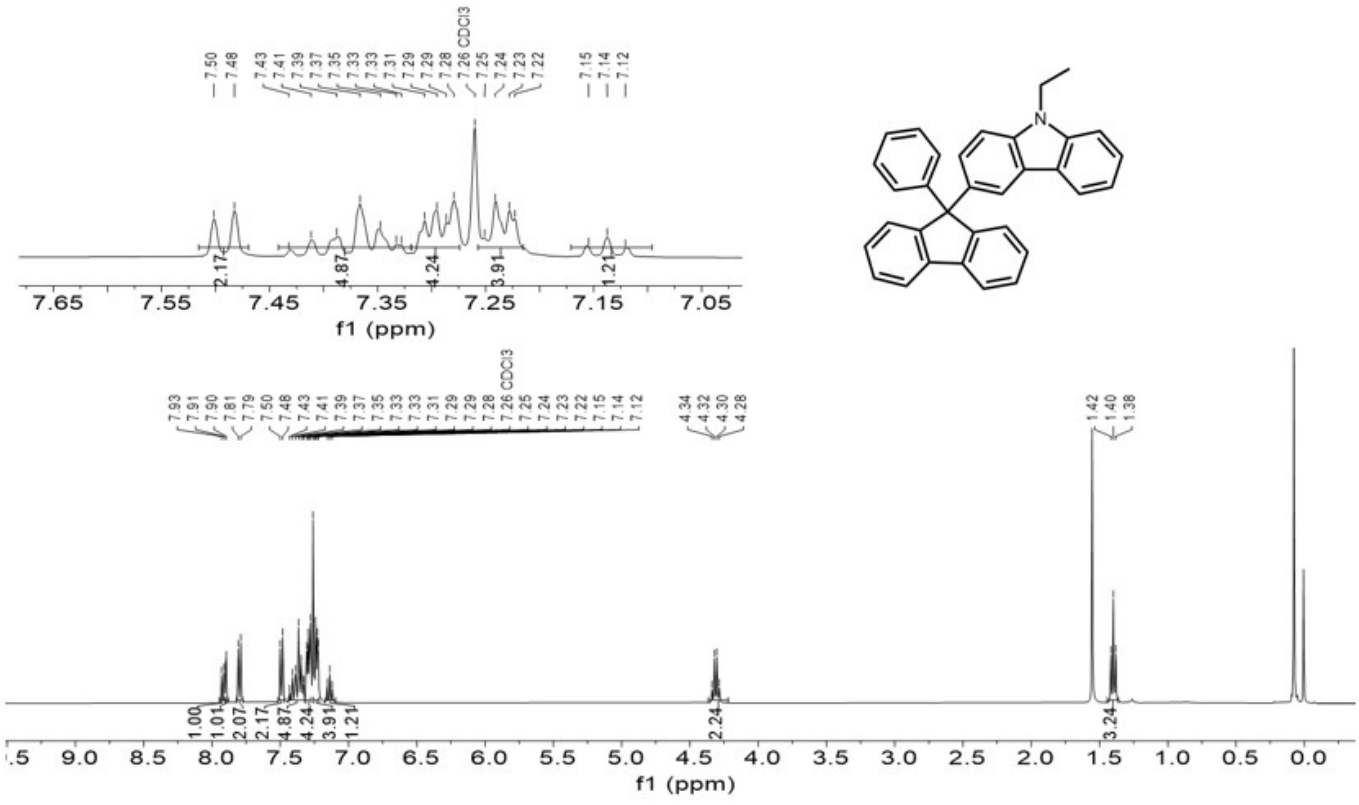

Figure S3. ^{1}H NMR spectrum of Et-PFCz recorded in $CDCl_3$.

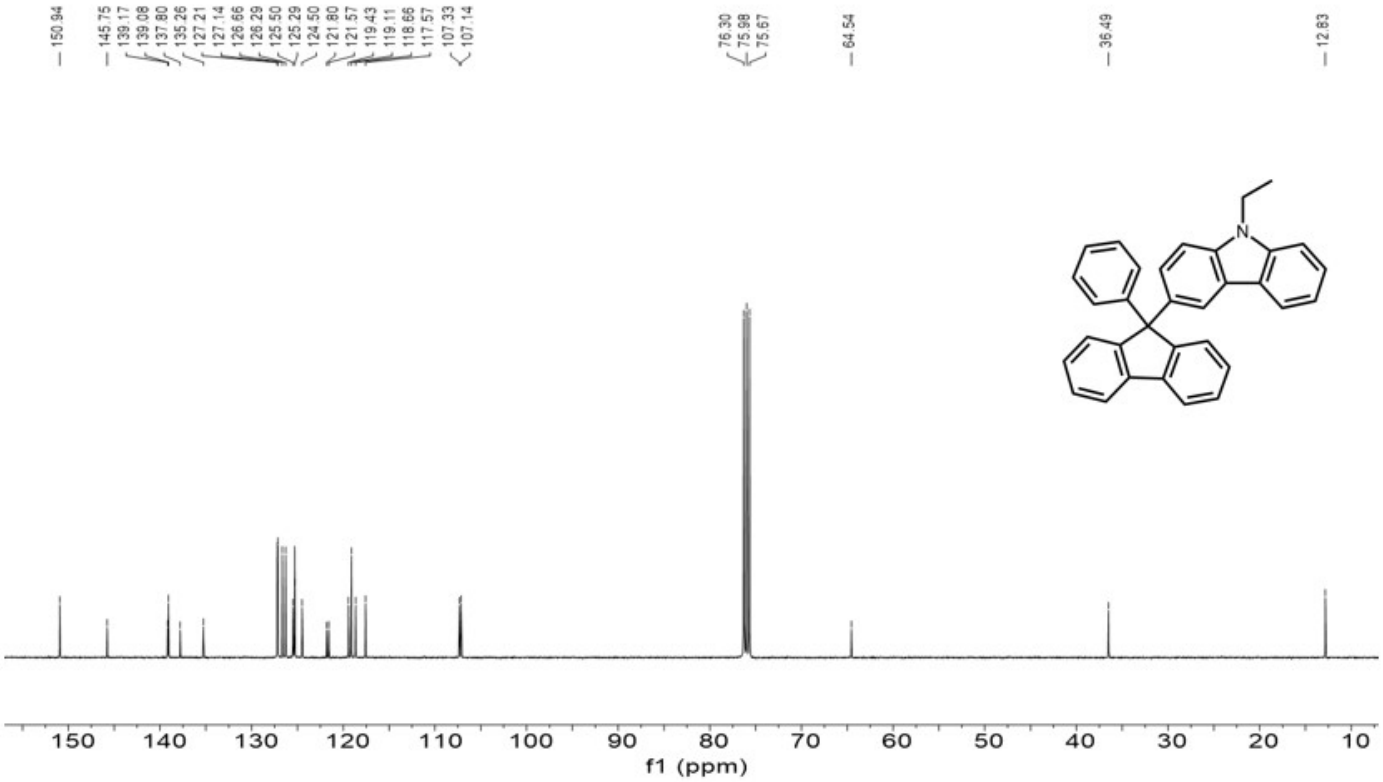

Figure S4. ^{13}C NMR spectrum of Et-PFCz recorded in $CDCl_3$.

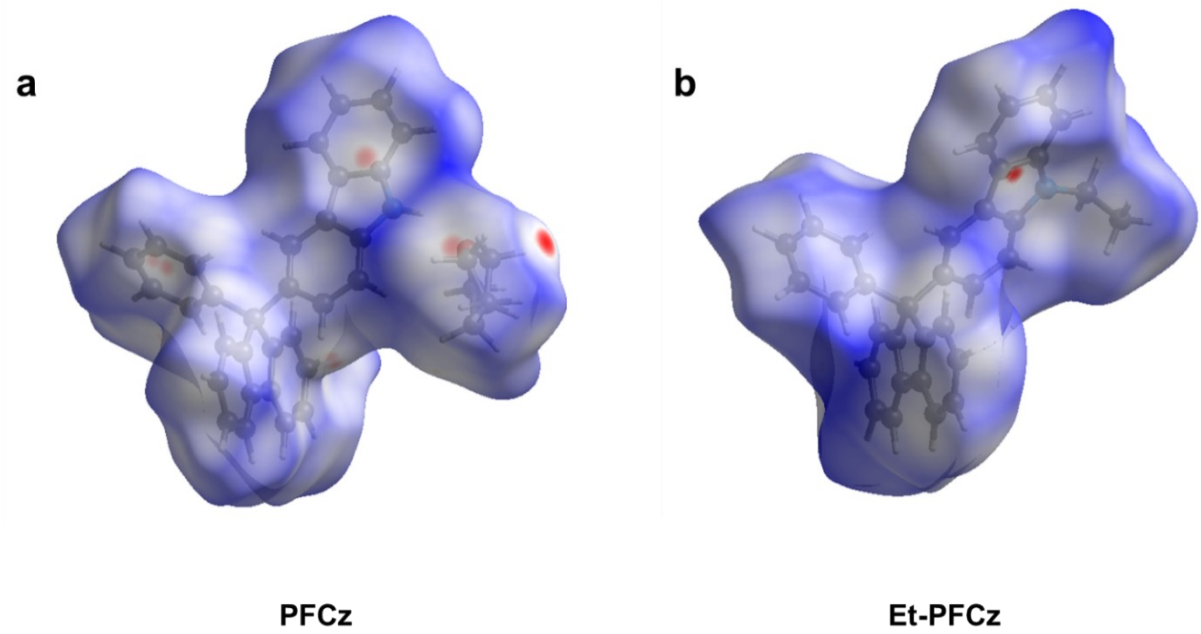

Figure S5. Hirshfeld surface maps showing supramolecular interaction sites of (a) PFCz and (b) Et-PFCz molecules.

Table S1. Crystal data for PFCz and Et-PFCz single crystals.

Name	PFCz	Et-PFCz
CCDC number	2495292	2495293
formula	$C_{31}H_{21}N$	$C_{33}H_{25}N$
space group	P 2_1/n	P b c a
lattice type	monoclinic	orthorhombic
a [Å]	15.2065(10)	16.4880(18)
b [Å]	10.9860(7)	8.6581(9)
c [Å]	15.9067(9)	33.176(3)
α [°]	90	90
β [°]	107.571(4)	90
γ [°]	90	90
V [Å^3]	2533.37	4736.03
Z	4	8
ρ_{calc} [g/cm^3]	1.257	1.222

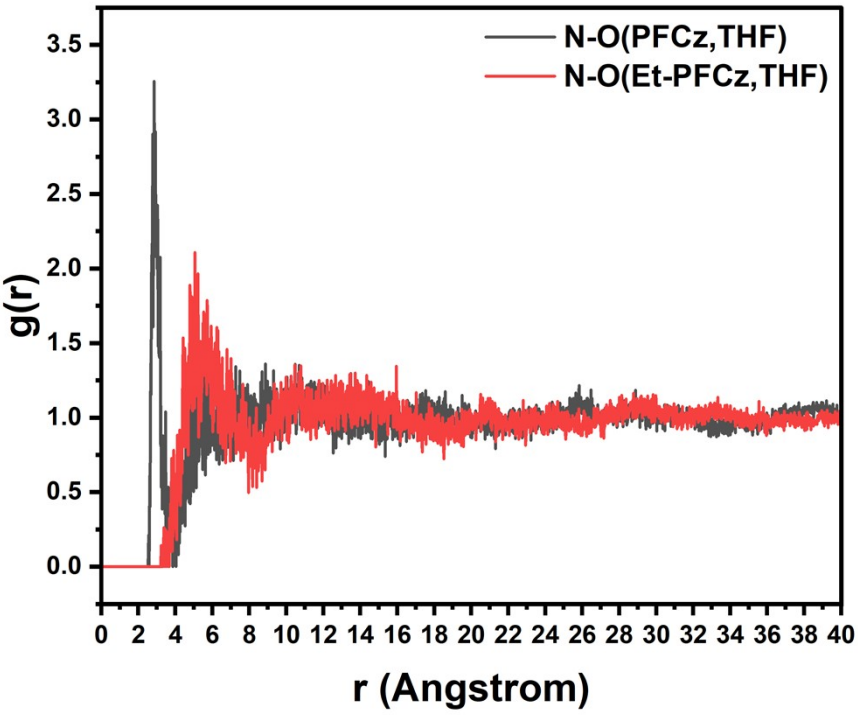

Figure S6. Radial distribution function, g(r), between the N atom of carbazole and the O atom of tetrahydrofuran. A pronounced peak at ~3 Å in the PFCz-THF system indicates a well-defined intermolecular interaction.

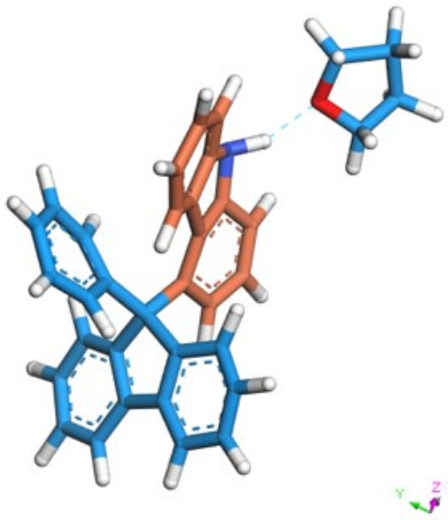

E(PFCz) (Ha)	-1247.078092
E(THF) (Ha)	-232.127681
E(PFCz-THF) (Ha)	-1479.215779
E (Ha)	-0.010006
E (kJ/mol)	-26.270753

Figure S7. Representative intermolecular packing geometry in the PFCz-THF system. The binding energy was calculated according to: E = E(PFCz–THF) – E(PFCz) – E(THF).

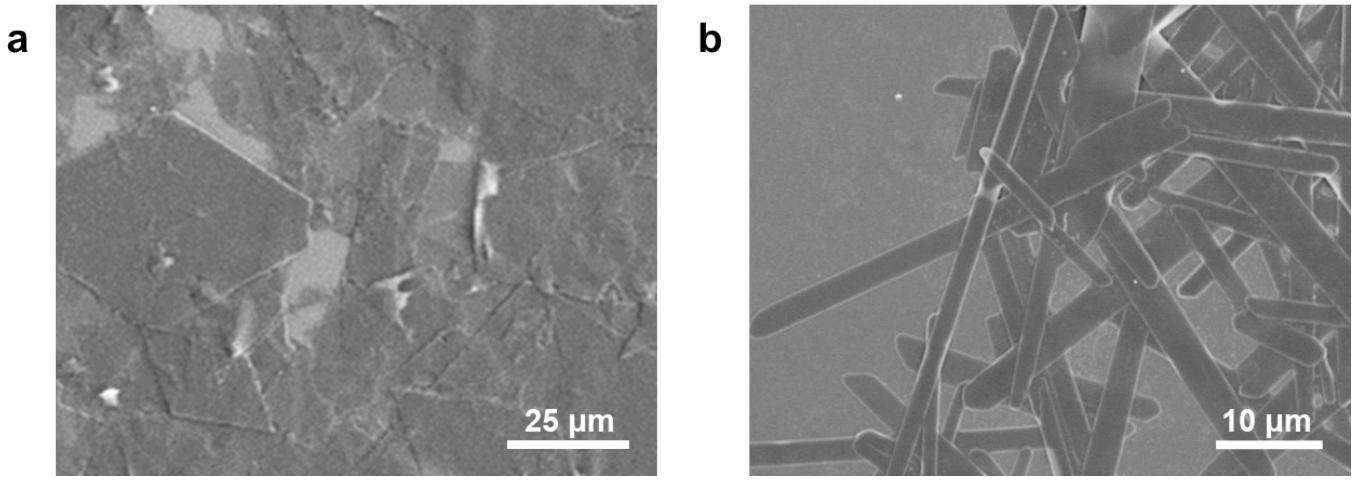

Figure S8. SEM images of (a) PFCz and (b) Et-PFCz microcrystals.

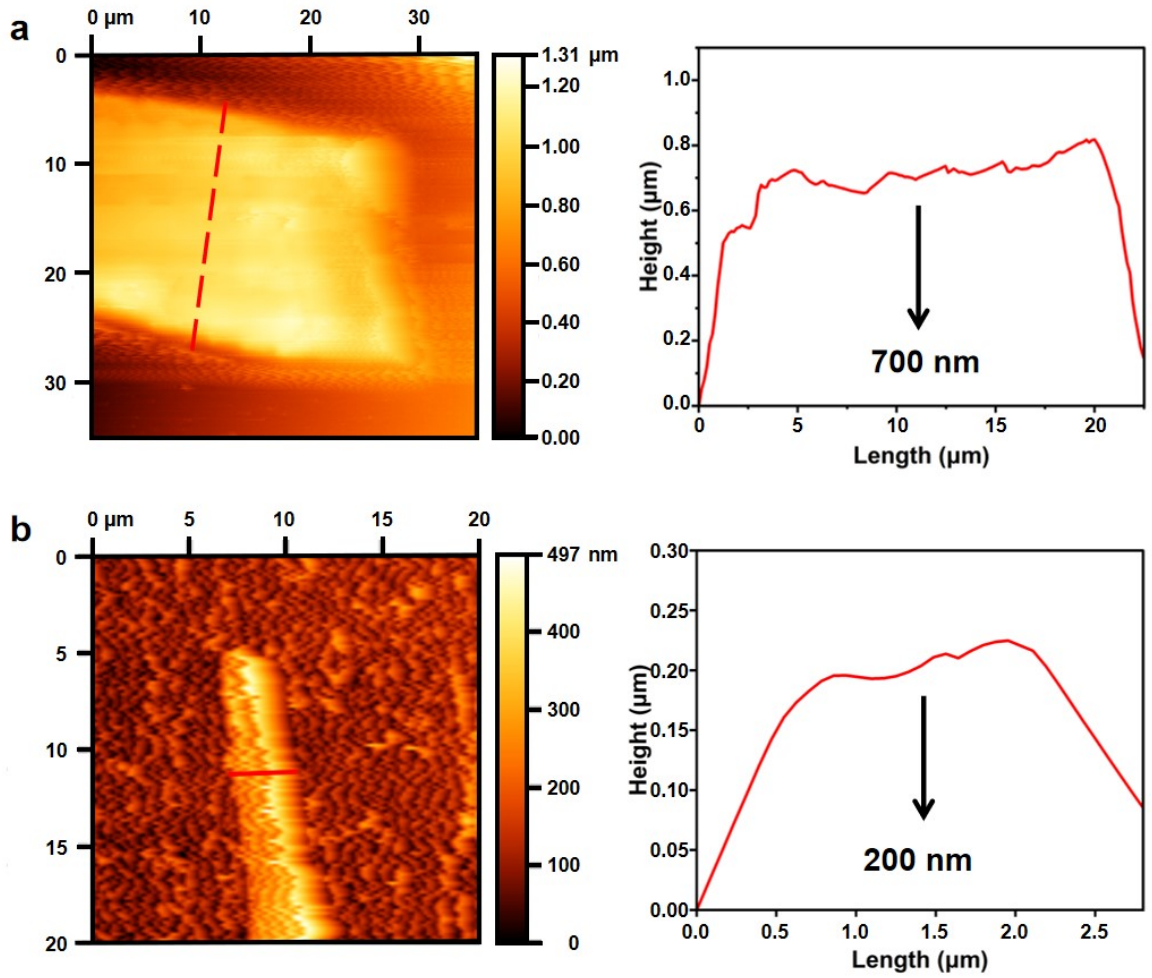

Figure S9. AFM images of (a) PFCz and (b) Et-PFCz microcrystals, along with their corresponding height profiles.

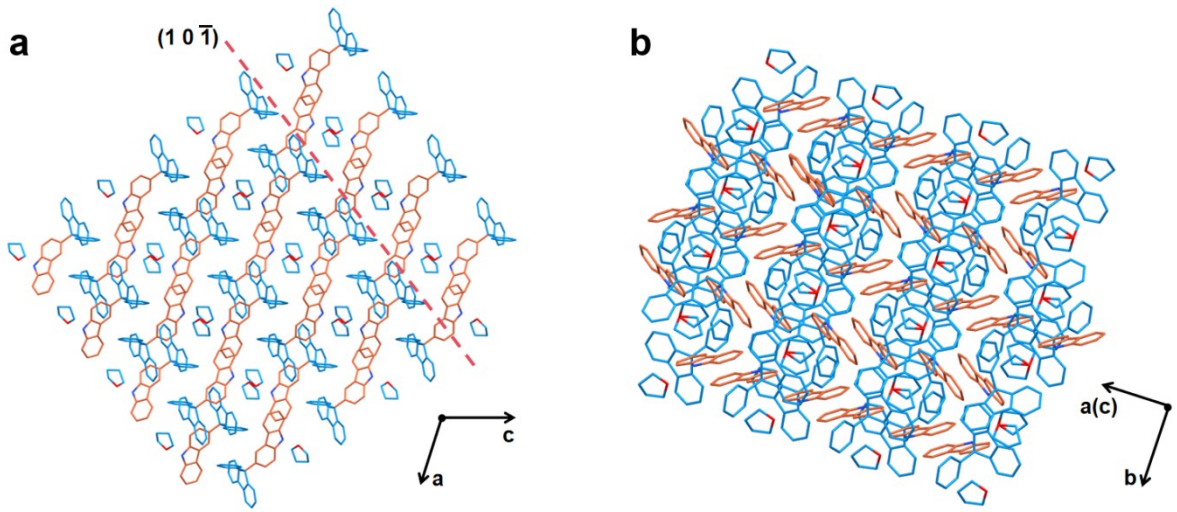

Figure S10. Molecular packing patterns of the PFCz crystal viewed along the [010] axis (a) and the [10$\bar{1}$] axis (b).

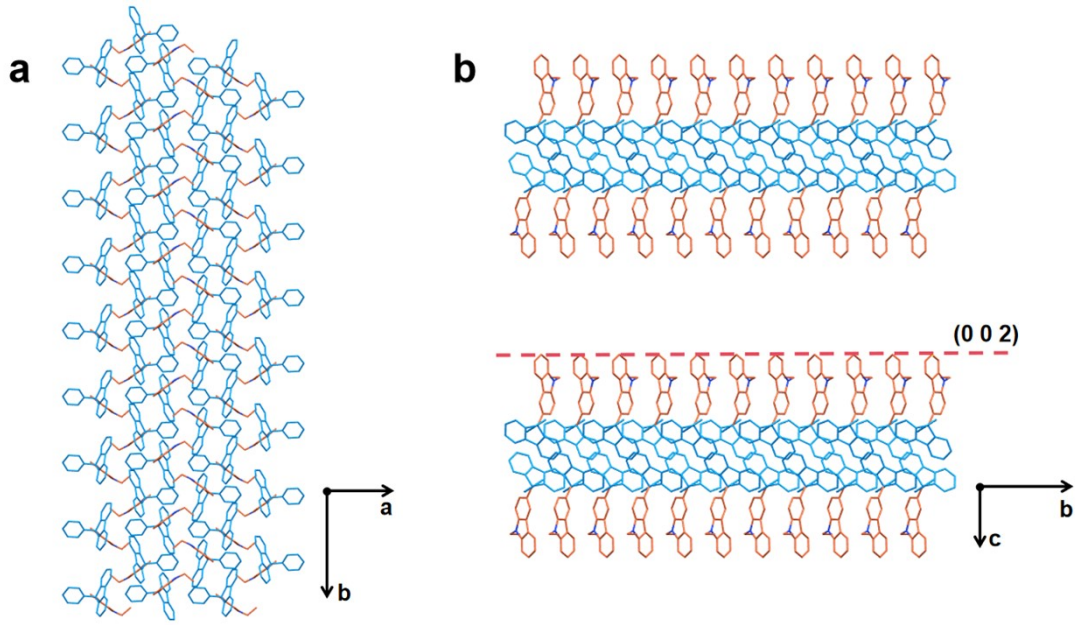

Figure S11. Molecular packing patterns of the Et-PFCz crystal viewed along the [001] axis (a) and the [100] axis (b).

Table S2. Comparison of the d-spacing and monolayer thicknesses of PFCz and Et-PFCz crystals.

Sample	n	λ	θ[a]	Calculated d-spacing[b]	Monolayer thickness[c]
PFCz	1	1.54050 Å	3.53°	1.251 nm	1.253 nm
Et-PFCz	2	1.54050 Å	2.66°	3.319 nm	3.318 nm

[a] The Bragg angles (θ) were obtained from the PXRD patterns of PFCz and Et-PFCz microcrystals (Fig. 2e and 2f).

[b] The d-spacing values were calculated according to the Bragg equation: $n\lambda = 2d\sin\theta$.

[c] The monolayer thicknesses were determined from the molecular packing patterns of PFCz and Et-PFCz (Fig. 3e and 3f).

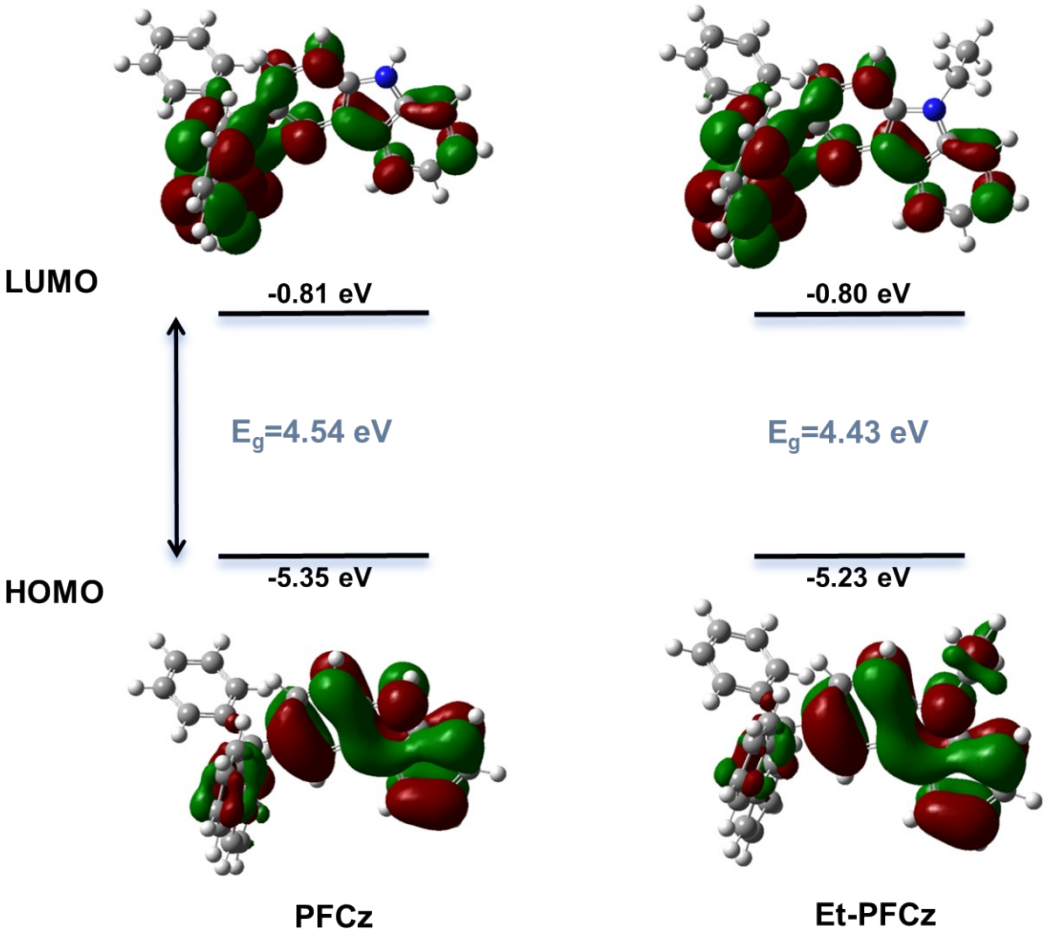

Figure S12. HOMO and LUMO distributions of PFCz and Et-PFCz single molecules calculated by DFT at the B3LYP/6-31G (d) level.

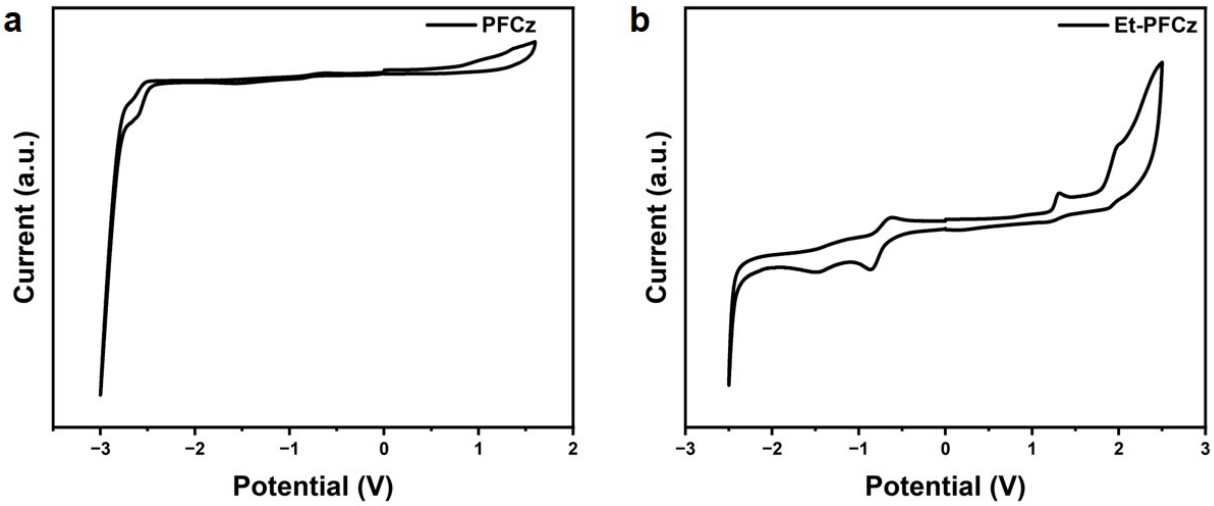

Figure S13. Cyclic voltammograms (CV) curves of PFCz (a) and Et-PFCz (b) under N_2.

Table S3. Comparison of PLQY values for molecular systems analogous to PFCz and Et-PFCz.

Molecule	Solution	Crystal Film	Reference
PF-Py	45	55	*Dyes Pigm.*, **2026**, *245*, 113259
SFX-2-Cz	50	31	*J. Phys. Chem. C*, **2021**, *125*, 6249−6259
SFX-2,7-DCz	84	51	
SO-Cz	10.6	7.9	*ACS Appl. Mater. Interfaces*, **2021**, *13*, 44615−44627
SON-Cz	37.5	19.7	
SON-PhCz	51.4	46.5	
1a-TPE-CN-Cz	/	41	*Small*, **2016**, *12*, 6554−6561
1b-TPE-CN-Cz	/	65	
1c-TPE-CN-Cz	/	56	
1d-TPE-CN-Cz	/	40	
PFCz	45.90	27.83	**This work**
Et-PFCz	47.57	52.21	

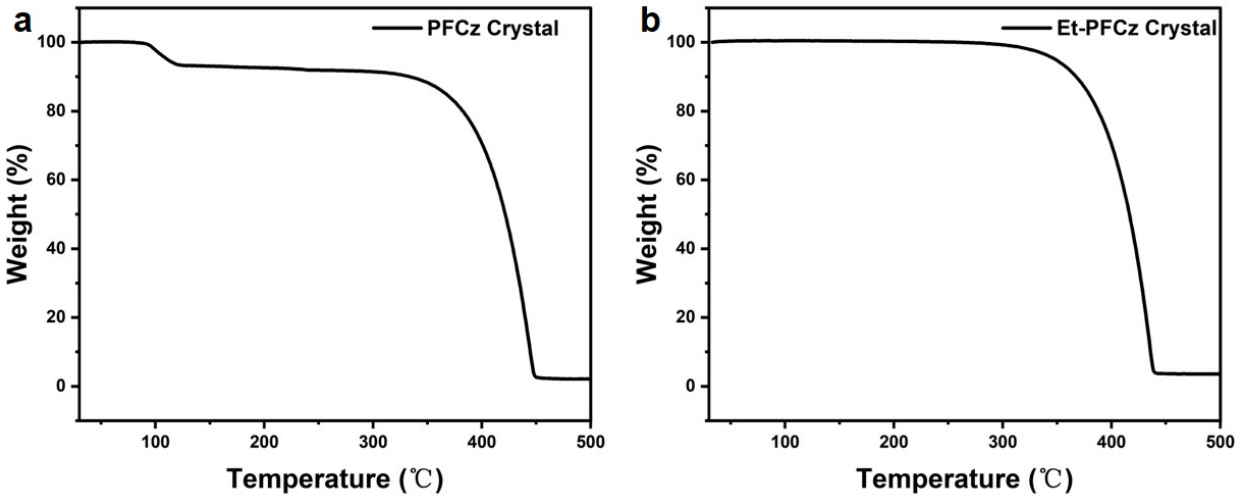

Figure S14. Thermogravimetric analysis (TGA) curves of PFCz (a) and Et-PFCz (b) microcrystals. Heating rate: 10 °C/min, nitrogen atmosphere.

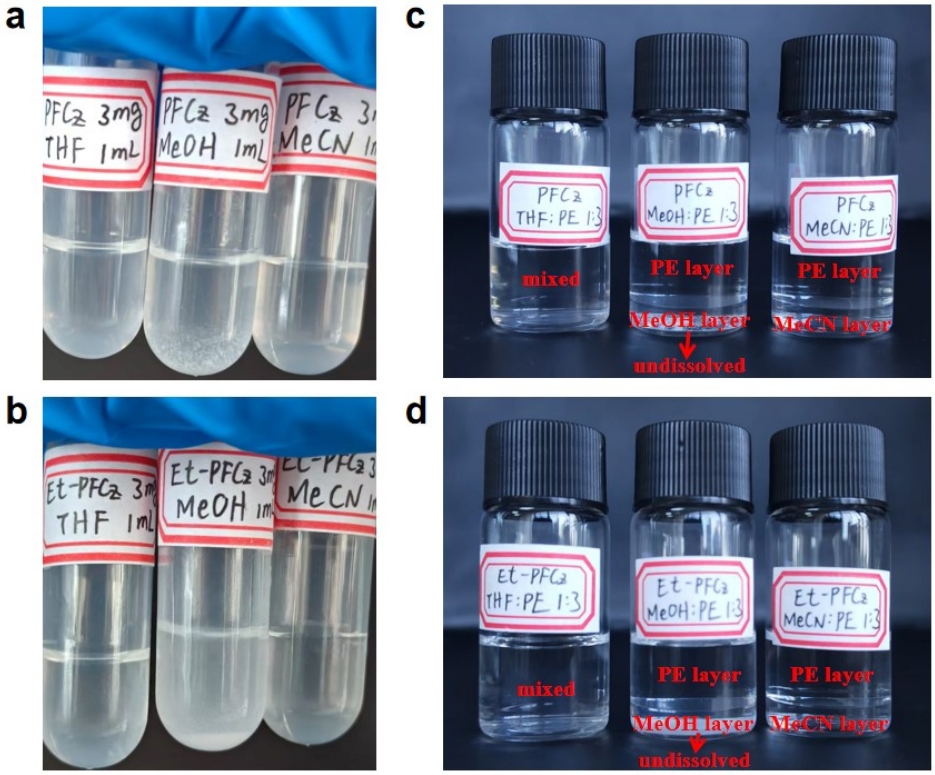

Figure S15. Dissolution state of PFCz (a) and Et-PFCz (b) in THF (left), MeOH (middle), and MeCN (right), and the miscibility state of PFCz (c) and Et-PFCz (d), respectively, in THF (left), MeOH (middle), and MeCN (right) upon addition of the poor solvent PE.

Single crystals of PFCz and Et-PFCz were grown via the solvent diffusion method, wherein the mutual diffusion between good solvent and poor solvent reduces the solubility of the target molecules, thereby achieving the growth of high-quality single crystals. We selected THF, MeOH, and MeCN as solvents for the experiments. As shown in Fig. S15a and S15b, even after prolonged sonication, PFCz and Et-PFCz remained undissolved in MeOH solution, precluding the growth of single crystals from MeOH. Subsequently, petroleum ether was introduced as a poor solvent. As shown in Fig. S15c and S15d, distinct phase separation was observed between the MeCN solutions of PFCz/Et-PFCz and petroleum ether, preventing mutual diffusion and the consequent reduction in solubility required for crystal growth. Therefore, single crystals could not be obtained from MeCN either. Ultimately, THF was selected as the optimal good solvent for dissolving PFCz and Et-PFCz to achieve successful single crystal growth.

Table S4. PLQY measurement conditions for PFCz in solution, amorphous film, and microcrystal film states.

PFCz		Solution	Amorphous Film	Microcrystal Film
Excitation Wavelength		300.00 nm	300.00 nm	300.00 nm
Emission Wavelength	Start	315.00 nm	315.00 nm	315.00 nm
	Stop	500.00 nm	500.00 nm	500.00 nm
Step		0.500 nm	0.500 nm	0.500 nm
Excitation Bandwidth		5.00 nm	5.00 nm	5.00 nm
Emission Bandwidth		0.30 nm	0.30 nm	0.30 nm
Dwell Time		0.200 s	0.200 s	0.200 s
Repeats		2	2	2
Temperature		-50.00 ℃	-50.00 ℃	-50.00 ℃
Excitation Correction		off	off	off
Reference Correction		on	on	on
Emission Correction		on	on	on

Table S5. PLQY measurement conditions for Et-PFCz in solution, amorphous film, and microcrystal film states.

Et-PFCz		Solution	Amorphous Film	Microcrystal Film
Excitation Wavelength		300.00 nm	300.00 nm	300.00 nm
Emission Wavelength	Start	315.00 nm	315.00 nm	315.00 nm
	Stop	500.00 nm	550.00 nm	550.00 nm
Step		0.500 nm	0.500 nm	0.500 nm
Excitation Bandwidth		5.00 nm	5.00 nm	5.00 nm
Emission Bandwidth		0.30 nm	0.30 nm	0.30 nm
Dwell Time		0.200 s	0.200 s	0.200 s
Repeats		2	2	2
Temperature		-50.00 ℃	-50.00 ℃	-50.00 ℃
Excitation Correction		off	off	off
Reference Correction		on	on	on
Emission Correction		on	on	on

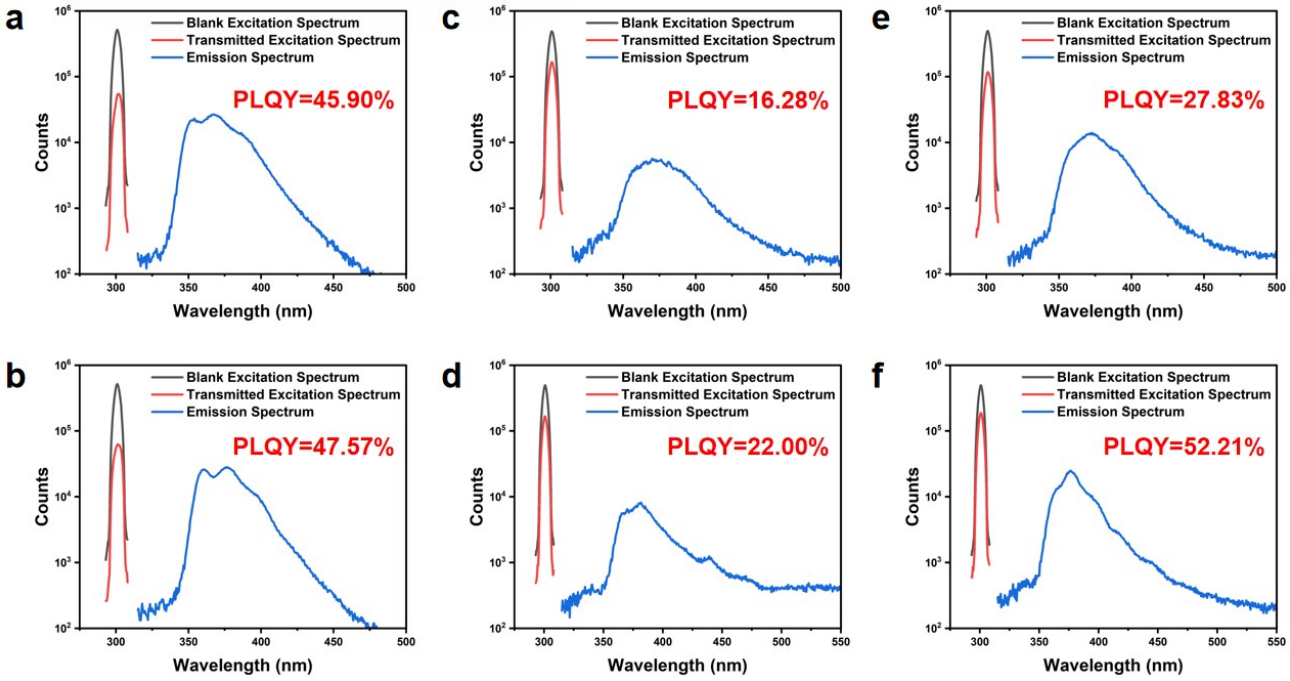

Figure S16. Direct method of PLQY measurements of PFCz (a,c,e) and Et-PFCz (b,d,f) in solution (a,b), amorphous film (c,d), and microcrystal film (e,f) states.